J Physiol 587.11 (2009) pp 2473–2485

The Journal of Physiology

Remodelling of the respiratory network in a mouse model of Rett syndrome depends on brain-derived neurotrophic factor regulated slow calcium buffering

S. L. Mironov[1,2], E. Skorova[1,2], N. Hartelt[1,2], L. A. Mironova[1,2], M. T. Hasan[3] and S. Kügler[1,4]

[1] *DFG-Center of Molecular Physiology of the Brain, Humboldtallee 23, 37073 Göttingen, Germany*
[2] *Department of Neuro- and Sensory Physiology, Georg-August-University, Humboldtallee 23, 37073 Göttingen, Germany*
[3] *Max Planck Institute for Medical Research, Jahnstr. 29, 69120 Heidelberg, Germany*
[4] *Department of Neurology, Georg-August-University, Waldweg 33, 37073 Göttingen, Germany*

Rett syndrome caused by MeCP2 mutations is a devastating neurodevelopmental disorder accompanied by severe breathing irregularities. Using transduction of organotypic slices from model MeCP2–/y mice with neuron-specific calcium sensor protein D3cpv, we examined the slow calcium buffering in neurons in pre-Bötzinger complex (preBötC), a component of the complex respiratory network. Examination of wild-type (WT) and MeCP2 null mice showed clear differences in the spatial organisations of neurons in preBötC and also in the disturbances in calcium homeostasis in mutant mice during early postnatal development. Deregulated calcium buffering in MeCP2–/y neurons was indicated by increased amplitude and kinetics of depolarisation-induced calcium transients. Both effects were related to an insufficient calcium uptake into the endoplasmic reticulum that was restored after pretreatment with brain-derived neurotrophic factor (BNDF). Conversely, the inhibition of BDNF signalling in WT neurons produced disturbances similar to those observed in MeCP2–/y mice. Brief hypoxia and calcium release from internal stores induced global calcium increases, after which the processes of many MeCP2–/y neurons were retracted, an effect that was also corrected by pretreatment with BDNF. The data obtained point to a tight connection between calcium homeostasis and long-term changes in neuronal connectivity. We therefore propose that calcium-dependent retraction of neurites in preBötC neurons can cause remodelling of the neuronal network during development and set up the conditions for appearance of breathing irregularities in Rett model mice.

(Received 27 January 2009; accepted after revision 30 March 2009; first published online 9 April 2009)
Corresponding author S. L. Mironov: Goettingen University, Neuro- und Sensory Physiology, Humboldtallee 23, Goettingen 37073, Germany. Email: smirono@gwdg.de

Abbreviations AAV, adeno-associated virus; BNDF, brain-derived neurotrophic factor; CCCP, carbonyl cyanide *m*-chlorophenyl hydrazone; DIV, days in vitro; ER, endoplasmic reticulum; FRET, fluorescence resonance energy transfer; KO, MeCP2–/y (null) mice; preBötC, pre-Bötzinger complex; RTT, Rett syndrome; SERCA, sarco/endoplasmic reticulum Ca^{2+}-ATPase; Tg, thapsigargin, trkB, tyrosine kinase B; WT, wild-type.

Rett syndrome (RTT) is a neurodevelopmental disorder primarily affecting young females, with an incidence of 1/10 000 to 1/15 000 live births (Francke, 2006; Chahrour & Zoghbi, 2007). RTT is caused primarily by mutations in MeCP2, which is a member of a family of proteins capable of binding to methylated DNA and recruiting chromatin-modifying activities that silence transcription. A loss of MeCP2 expression leads to a RTT-like phenotype including tremors, breathing irregularities and hypoactivity. Both in mouse (Larimore *et al.* 2009) and humans (Wenk, 1997), post-mortem RTT brains show a reduced brain size, a decrease in the size of individual neurons and a reduction of dendritic arborisation. Mouse models (Guy *et al.* 2001) have provided significant advances in the understanding of RTT and MeCP2 function (Viemari *et al.* 2005; Nelson *et al.* 2006; Wang *et al.* 2006; Zhou *et al.* 2006; Chao *et al.* 2007; Stettner *et al.* 2007; Fischer *et al.* 2008). Many similarities between Rett syndrome in mice and in humans thus can justify a frequently encountered point of view (cf. Gaultier & Gallego, 2008) that mutant newborn mice with targeted deletions of genes are a promising research object towards the development of new treatments for respiratory-control disorders in humans. Concerning Rett syndrome, there are also some differences between species, as discussed recently by Sun & Wu (2006), so that the extrapolation

DOI: 10.1113/jphysiol.2009.169805

of experimental results must be made with caution. Breathing pattern abnormalities often occur in mutant newborn mice lacking genes involved in the development and modulation of rhythmogenesis of the respiratory network; a component of the latter is the pre-Bötzinger complex (preBötC, Smith *et al.* 1991), represented by a compact formation of neurons in the lower brainstem (Feldman & Del Negro, 2006).

Recent studies also implicate an involvement of brain-derived neurotrophic factor (BDNF), a recently identified MeCP2 target, in the development of RTT both in mice (Chen *et al.* 2003; Zhou *et al.* 2006; Ogier *et al.* 2007; Larimore *et al.* 2009) and in humans (Francke, 2006; Nectoux *et al.* 2008). BDNF is a neurotrophin required for survival, growth and maintenance of neurons during development and is involved in learning and memory. BDNF modulates synaptic plasticity (Bramham & Messaoudi, 2005; Turrigiano, 2007). Many of its actions are mediated by tyrosine kinase B (trkB) receptors (Martinowich *et al.* 2007). Neurons in MeCP2 null mice express significantly lower levels of BDNF (Ogier *et al.* 2007) that may negatively influence synaptogenesis, the latter being thought to be completed within the first 2 weeks of postnatal development in mice (Zoghbi, 2003). Up to now the molecular effects of BDNF on the development of neuronal circuitry in RTT mice have not been identified. MeCP2 null mice show distinct signs of breathing disturbances (Viemari *et al.* 2005; Stettner *et al.* 2007) that can be related to BDNF, with trkB receptors that are important in the generation of the respiratory rhythm (Bouvier *et al.* 2008).

The actions of Ca^{2+} as second messenger are versatile (Berridge *et al.* 2000) and Ca^{2+} plays an important role in generating rhythmic activity in the respiratory network (Mironov, 2008, 2009). Acting as a second messenger, Ca^{2+} also represents a crucial factor in neuronal development (Spitzer *et al.* 2002; Wong & Ghosh, 2002; Ciccolini *et al.* 2003; Henley & Poo, 2004; Hua *et al.* 2005; McAllister, 2007). Aiming to study the role of Ca^{2+} in Rett syndrome, we expressed neuron-specific fluorescent sensor protein in organotypic brainstem slices containing preBötC. Wild-type (WT) and MeCP2 null mice (KO) showed a clearly different spatial organisation of neurons in preBötC and demonstrated disturbances in calcium homeostasis in mutant mice that were corrected by BDNF. In view of the data we thereby obtained, we propose that BDNF deficiency in RTT causes deregulation of the slow calcium buffering responsible for Ca^{2+} removal from the cytoplasm and that this deficiency also provokes spontaneous global calcium transients, triggering excessive retraction of neuronal processes. The resultant compromised wiring within the pre-Bötzinger complex can be responsible for the breathing irregularities observed in Rett syndrome in mice.

Methods

Ethical approval

All animals were housed, cared for and killed in accordance with the recommendations of the European Commission (No. L358, ISSN 0378-6978), and the protocols were approved by the Committee for Animal Research, Göttingen University.

Preparation

Experiments were performed using the mouse model for Rett syndrome, strain B6.129P2(C)-MeCP2tm1-1Bird (Guy *et al.* 2001). The mice were obtained from the Jackson Laboratory (Bar Harbor, ME, USA) and maintained on a C57BL/6J background. Hemizygous mutant *MeCP2−/y* males (denoted henceforth as KO mice) were generated by crossing heterozygous *MeCP2*+/− females with C57BL/6J WT males. Before experiments, all mice were routinely genotyped in accordance with the Jackson Laboratory genotyping protocols as described by Stettner *et al.* (2007).

Organotypic culture slices were obtained as described previously (Hartelt *et al.* 2008); they possessed pertinent anatomical hallmarks characteristic for the transverse section of the brainstem containing preBötC (Ruangkittisakul *et al.* 2006). The animals were prepared at postnatal day (P) 2–P4 and P18–P20 (denoted henceforth as P3 and P19, respectively). Slices after preparation were placed on the support membranes (Millicell-CM Inserts, PICMORG50; Millipore) and 1 ml medium was added so as to expose the surface of the slice continuously to the incubator gas mixture. The medium (50 % minimal essential medium (MEM) with Earle's salts, 25 mM Hepes, 6.5 mg ml^{-1} glucose, 25% horse serum, 25% Hanks' solution buffered with 5 mM Tris and 4 mM $NaHCO_3$, pH 7.3) was changed every 2 days. All chemicals were from Sigma (Deisenhofen, Germany).

Preparations from P3 mice were examined between 10 and 45 days *in vitro* (DIV), corresponding to postnatal days P14–P49. The animals were examined in groups at the interval of 1 week starting from P14. Approximately equal numbers of neurons from the respective groups were measured in parallel. All data were acquired and analysed blinded to genotype. Each test in this study was repeated with at least four different preparations and the mean data were obtained by analysing responses of 6–12 neurons in the image field.

Because the properties of neurons in culture may be modified during long-term incubation, we also prepared slices from P3 and P19 mice and examined them at the same postnatal day. Slices in the experiments were fixed on a coverslip mounted in the recording chamber and continuously superfused at 34°C with artificial cerebrospinal fluid (ACSF).

Calcium changes were examined by applying high-K^+ (5–10 s, the exchange time <1 s), 1 μM thapsigargin, carbonyl cyanide *m*-chlorophenyl hydrazone (1μM CCCP) and 200 μM KCN, 100 ng ml^{-1} BDNF (2 to 3 min) or 20 ng ml^{-1} BDNF, and 100 nM TrkB blocker K252a, ([methyl-9-(*S*)-12(*R*)-epoxy-1*H*-diindolo[1, 2, 3-fg:3′2′1′-kl]pyrrolo[3,4-i][1,6]benzodiazocine-2, 3, 9, 10, 11, 12-hexahydro-10-(*R*)-hydroxy-9-methyl-1-oxo-10-carboxilate) (20 min). High-K^+ solution was prepared by exchanging Na^+ in ACSF and all other testing solutions were produced by adding aliquots of corresponding stock solutions directly to ACSF. In order to examine the long-term effects of BDNF, we supplied the culture medium with 10 ng ml^{-1} BDNF. The slices from the control and mutant mice were examined in parallel.

Imaging

Intracellular calcium was measured using calcium sensor D3cpv (Palmer *et al.* 2006; Palmer & Tsien, 2006; Wallace *et al.* 2008). In order to obtain a neuron-specific transduction (Kügler *et al.* 2003; Shevtsova *et al.* 2005) the sensor was embedded in a recombinant adeno-associated virus (AAV) vector. For transduction, we applied 1 μl of AAV solution ($\sim 1 \times 10^9$ viral genomes) directly onto the slice surface. The expression of D3cpv was detectable 2 days after transduction, reached a steady state after 4–6 days and then remained constant over 6 weeks.

The optical recording system was based on a Zeiss Axioscope. D3cpv was excited at 430 nm by the light generated by LED (20 mW, Roithner Lasertechnik). Free calcium levels were obtained by rationing the emission of cyan fluorescent protein (CFP) at 470 nm to FRET signal between CFP and yellow fluorescent protein (YFP; emitted at 535 nm). Corresponding signals were separated with Optosplit (BFI Optilas, Puchheim, Germany) using dichroic mirror (495 nm) and 470 ± 12 and 535 ± 15 nm filters. Images were captured by a cooled CCD camera (ANDOR, Offenbach, Germany) and collected with ANDOR software (500×500 pixels at 12 bit resolution). Fluorescence signals were analysed offline with a MetaMorph software (Princeton Instruments, Sunnyvale, CA, USA). Cytoplasmic calcium levels were obtained from ratios of FRET and CFP signals (R) using the formula

$$[Ca^{2+}]_i = \frac{R - R_{min}}{R_{max} - R}$$

first derived for fura-2 (Grynkiewicz *et al.* 1985). The dissociation constant $K_d = 0.6$ μM was taken from Palmer *et al.* (2004) and the values of $R_{min} = 1$ and $R_{max} = 80$ were determined with ionomycin (Palmer *et al.* 2006). D3cpv was chosen over other imaging dyes such as fura-2 not only because it can be selectively expressed in neurons but also for its other advantages such as its greater dynamic Ca^{2+} detection range (0.6–6 mM) and its greater resistance to photobleaching, allowing us to image cells for about 1 h without significant deterioration of fluorescence.

Results

Distorted topology of the network in preBötC in MeCP2 KO mice

The low-resolution ($\times 10$) image of a transverse brainstem slice transduced with the neuron-specific fluorescent Ca^{2+}-sensor D3cpv shown in Fig. 1*A* demonstrates the organisation of neurons in the transverse slice and location of preBötC. At higher resolution the neurons and their processes had their typical appearance (Fig. 1*B* and *C*) closely resembling that obtained previously in slices transduced with adenovirus (AAV) construct containing green fluorescent protein (GFP) and synapsin I promoter (Hartelt *et al.* 2008). Notably, imaging of virally delivered calcium sensor in the slice revealed fine details of neuronal processes that sharply contrast with the blurred images of fura-2 in slices (Hartelt *et al.* 2008). Because the sensor is based on a strictly neuronal promoter, it completely filled the interior of neurons after expression and only slight regional variations were present. For analysis of network wiring we needed contiguous images of neurons and produced them by appropriate thresholding of the pictures as shown in the insets in Fig. 1*B*. These binary images were used to generate the wiring diagrams by applying previously described algorithms (Hartelt *et al.* 2008).

The morphology of neurons and their organisation in the pre-Bötzinger complex in wild-type mice did not change significantly within the first two postnatal months but the network in KO mice apparently reorganized during this time period (Fig. 1*C*). In the KO mice, the number of neurons (Fig. 2*A*) and connections between them (Fig. 2*B*) were already significantly smaller at P14 (corresponds to 11 DIV) and the differences between WT and KO became even bigger at later examination times. KO neurons had smaller dimensions (mean diameter 14.1 ± 1.2 *vs.* 19.2 ± 1.4 μm at P28, $n = 64$, $P < 0.05$), which, among other morphological features, represents a hallmark of Rett syndrome both in mice (Larimore *et al.* 2009) and in humans (Wenk, 1997).

These changes cannot be related to the differential expression of D3cpv in WT and KO preparations, because all slices were transduced during the first postnatal week and the neurons in slices maintained production of the sensor at all times in the culture. The culture conditions may, however, have influenced WT and KO neurons differentially during maturation. To exclude such a possibility, we prepared the slices from both types of mice at P19 and repeated the measurements. Appearances of

slices in the two preparations and morphological data were similar at the same postnatal day as indicated by the middle part of the bar graphs in Fig. 2 where the data obtained in P3 and P19 slices overlap. This justifies the absence of particular changes in the developmental programme in culture as factors in the differences between wild-type and KO mice. Rett syndrome is currently connected with a deficiency in BDNF production and secretion (see Introduction). When the slices derived from P3 KO mice were cultured in the presence of 10 ng ml^{-1} BDNF, the number of neurons and connections showed no significant differences from those in WT mice (Fig. 2*A*, *B*) indicating a positive influence of BDNF during the maturation of KO slices.

The above changes observed in the developmental programme of the 'Rett' mice could be caused by intracellular calcium, because its resting values were higher in all KO preparations examined and they were corrected to

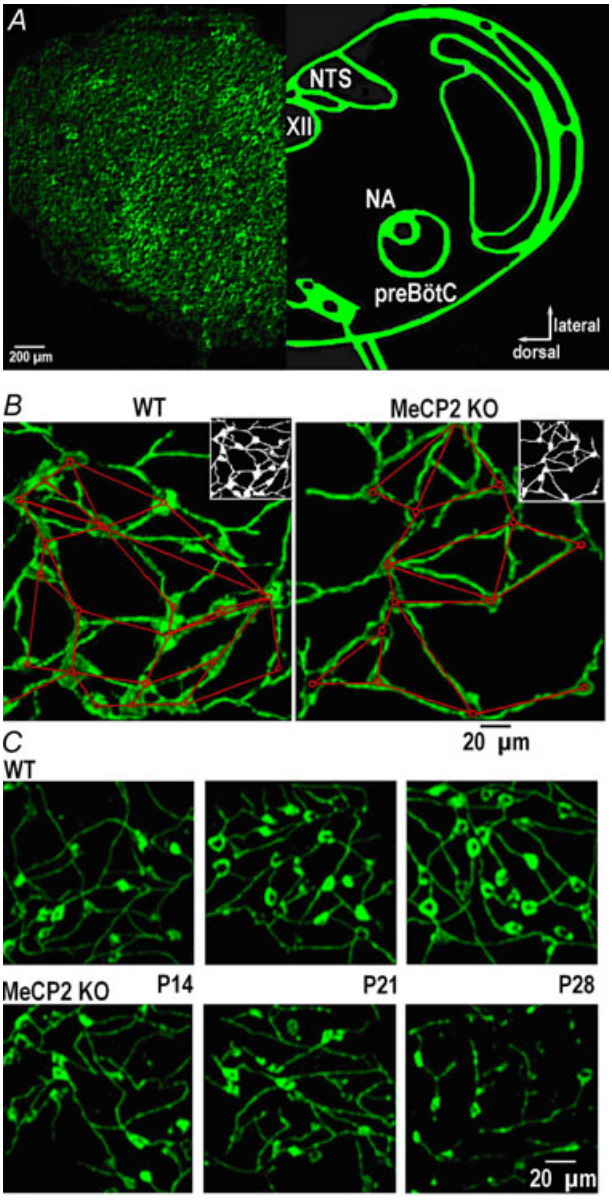

Figure 1. Topology of the respiratory network and its modification in MeCP2 KO mice
A, left, image of the transverse WT slice at P28 transduced with AAV-D3cpv; right, schematic presentation of main anatomical nuclei in this brainstem section (NA, nucleus ambiguus; XII, nucleus hypoglossus; NTS, nucleus tractus solitarii; preBötC, pre-Bötzinger complex). *B*, part of preBötC region in wild-type (WT) and *MeCP2–/y* (KO) mice at P21. The binary images shown in right upper insets were used to obtain the wiring diagrams within a network; its nodes (the cell bodies) are indicated by circles; the lines approximate interconnecting neural processes and represent the edges of the network. In these two images of WT (KO) networks we counted 20 (14) nodes and 25 (18) edges. *C*, typical appearances of the preBötC region at different postnatal days in WT and KO mice.

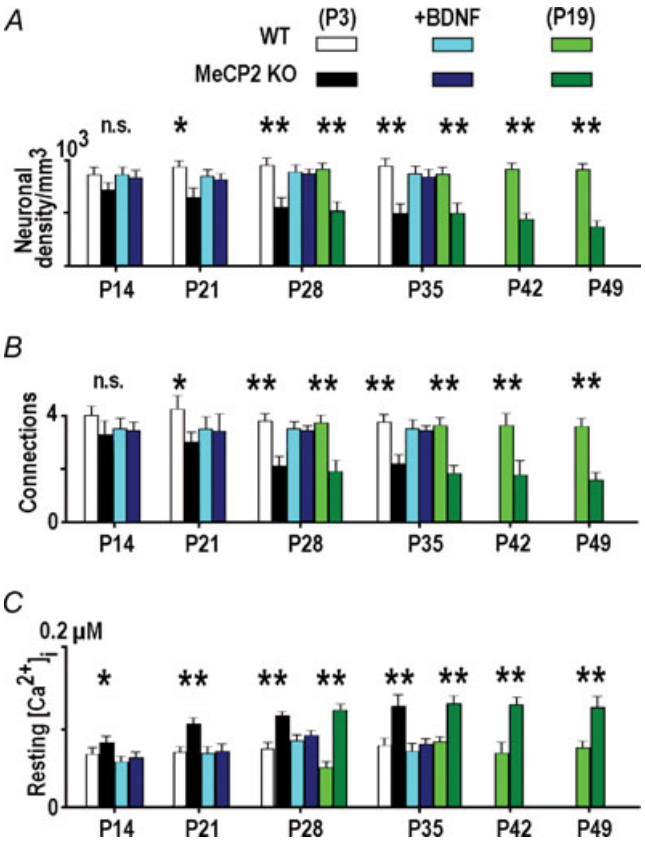

Figure 2. Some characteristics of preBötC neurons in WT and MeCP2 KO mice
Bar graphs show the density of neurons in preBötC (*A*), mean number of interneuronal connections (*B*), and resting calcium levels (*C*) in different age groups of wild-type and MeCP2 KO mice. The data were obtained in mice prepared at P3 and P19 and examined at the times indicated. We also examined preparations derived from P3 mice which were maintained in culture in the presence of 10 ng ml^{-1} BDNF. Note the similarity between the mean values obtained in slices from P3 and P19 mice examined at the same postnatal days (the middle parts of the bar graphs) and the positive effects of incubation of KO slices in the presence of BDNF. Significance levels: non-significant (n.s.), $P < 0.05$ (*), $P < 0.01$ (**). The data were collected in 4–6 different preparations.

the normal values by BDNF (Fig. 2*C*). Elevated resting $[Ca^{2+}]_i$ levels point to particular disturbances in calcium homeostasis in KO neurons that could be responsible for the long-term changes observed in the morphology of neurons and their connectivity.

Impaired Ca^{2+} homeostasis in MeCP2 KO neurons and its correction by BDNF

Resting $[Ca^{2+}]_i$ is normally controlled by the processes that are collectively referred to as slow Ca^{2+} buffering. They include specific transport systems in the endoplasmatic reticulum (ER), mitochondria and plasma membrane. Because all participating systems are also active at rest, any changes in basal $[Ca^{2+}]_i$ levels should indicate modification of one or more of these. Slow buffering of Ca^{2+} is best examined by analysing the amplitude and time course of the depolarisation-evoked calcium transients. At first approximation (Mironov, 1995), the rate constant of $[Ca^{2+}]_i$ recovery from the steady state ($=1/\tau$ where τ is the time constant) is a sum of rate constants of all participating systems and the maximal amplitude (a new steady level attained during depolarisation) is determined by the product $J\tau$ where J is the Ca^{2+} influx into the cell.

Figure 3*A* shows calcium measurements in neurons which demonstrated periodic activity in the form of rhythmic calcium transients accompanying the bursts of action potentials in spontaneously active cells in this preparation (Hartelt *et al.* 2008). In KO neurons the transients had bigger amplitudes than in WT neurons (0.16 ± 0.02 *vs.* 0.09 ± 0.02 μM) and slower recovery time constants (5.1 ± 1.2 *vs.* 3.1 ± 0.8 s; the values are the means for 24 neurons of each sort). Depolarisation with high-K^+ evoked bigger transients that decayed more slowly (mean amplitudes and recovery time constants in WT and KO neurons were 0.25 ± 0.3 *vs.* 0.39 ± 0.4 μM and 6.1 ± 0.2 *vs.* 11.1 ± 0.2 s, respectively, $n = 24$). The difference in time constants for spontaneous and evoked calcium transients can be explained by shorter duration of spontaneous bursts, after which the recovery of $[Ca^{2+}]_i$ is faster, because initial levels do not attain homogeneous distribution in the cytoplasm and Ca^{2+} is additionally redistributed via diffusion after the Ca^{2+} influx ceases. Such effects depend on each cell's size and geometry and give variable contributions to the time constants. In order to exclude such effects, we analysed the kinetics of calcium recovery after 5 s-long depolarisations. The latter produced uniform steady $[Ca^{2+}]_i$ levels in the cytoplasm as indicated by distinct plateaus in Fig. 3*A* and subsequent figures. The changes in calcium levels and time constants of recovery between WT and KO neurons were not due to differential expression of D3cpv sensor or changes in its properties, because fluorescence signals recorded in both preparations had similar amplitudes and identical minimal and maximal values during calibration with ionomycin (see Methods).

Ca^{2+} uptake by mitochondria and ER was further examined by applying protonophore carbonyl cyanide *m*-chlorophenylhydrazone (CCCP), a respiratory chain uncoupler, and thapsigargin, a sarcoplasmic reticulum Ca^{2+}-ATPase (SERCA) inhibitor. Both agents released Ca^{2+} from the respective internal store and significantly increased both the peak amplitude and time constant of recovery after depolarisation (Fig. 4*A–D*, Table 1).

In neurons that were derived from WT and KO mice and maintained in culture in the presence of 10 ng ml^{-1} BDNF, the depolarisations-evoked calcium transients had identical time courses and amplitudes. The mean values at P28 were equal to 6.4 ± 0.5 *vs.* 7.1 ± 0.6 s and 0.26 ± 0.06

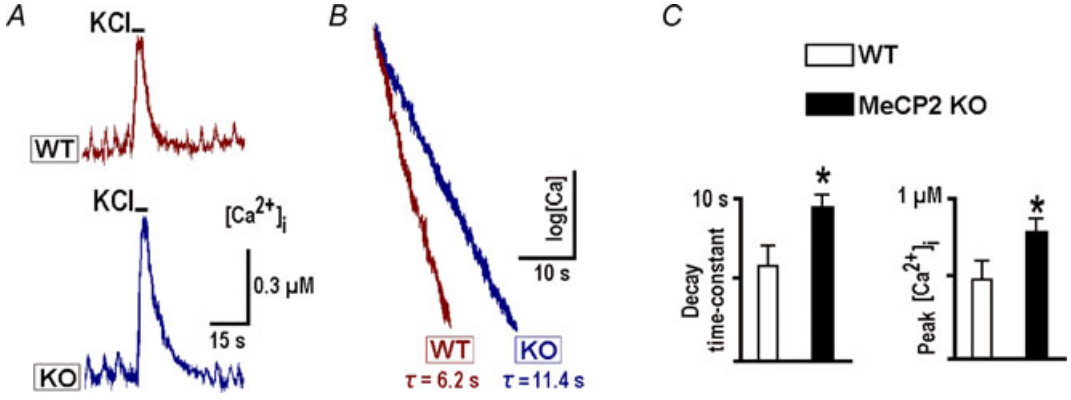

Figure 3. Calcium transients in wild-type and MeCP2 KO mice
A, typical depolarisation-induced calcium transients in spontaneously active preBötC neurons evoked by application of 50 mM K^+ for 5 s. *B*, the same transients are presented as semi-log plots to show the extended time course of decay in KO mice. *C*, mean decay time constants and peak increases during depolarisation, obtained in 6–8 different preparations at P21.

Table 1. Time constants of $[Ca^{2+}]_i$ recovery after membrane depolarisation and peak calcium levels after calcium release from mitochondria and ER in wild-type and MeCP2 mice

	Time constant (s)				$[Ca^{2+}]_i$ increase (μM)	
Animals	Before	After CCCP	Before	After Tg	CCCP	Tg
WT	6.8 ± 0.5	11.2 ± 1.2	6.5 ± 0.4	16.2 ± 1.5	0.33 ± 0.05	0.42 ± 0.04
KO	12.3 ± 0.4	25.4 ± 0.7	12.1 ± 0.5	29.2 ± 0.8	0.54 ± 0.07	0.31 ± 0.05
KO+BDNF	7.2 ± 0.6	13.4 ± 1.0	7.5 ± 0.5	18.4 ± 1.1	0.35 ± 0.04	0.44 ± 0.03
WT+K252a	11.3 ± 0.5	24.5 ± 0.6	11.4 ± 0.6	30.3 ± 0.9	0.51 ± 0.06	0.29 ± 0.04

Mean data $\pm$ S.E.M. were obtained in 15 to 25 neurons in four different preparations and are significant at $P < 0.01$. Responses of WT and KO neurons to membrane depolarisations were evaluated in a control and calcium release from mitochondria and ER with CCCP and thapsigargin, respectively. Experimental protocols were then repeated after pretreatment with BDNF (20 ng ml^{-1}) and TrkB blocker K252a (100 nM).

vs. 0.29 ± 0.07 μM ($n = 12$) in WT and KO, respectively, and the differences at P14 and P21 were also not significant. After incubation of KO slices with 20 ng ml^{-1} BDNF for 20 min, the responses to membrane depolarisation and calcium release also had amplitudes and decay times closer to those measured in WT (Fig. 4*E* and *F*; Table 1). Pretreatment of WT slices with the trkB blocker K252a produced opposite effects, and calcium transients acquired the form typical for KO neurons (Fig. 4*G*, *H*; Table 1). The specificity of trkB blockade was confirmed by applying the inactive analogue K-252b, which showed no effects ($n = 4$).

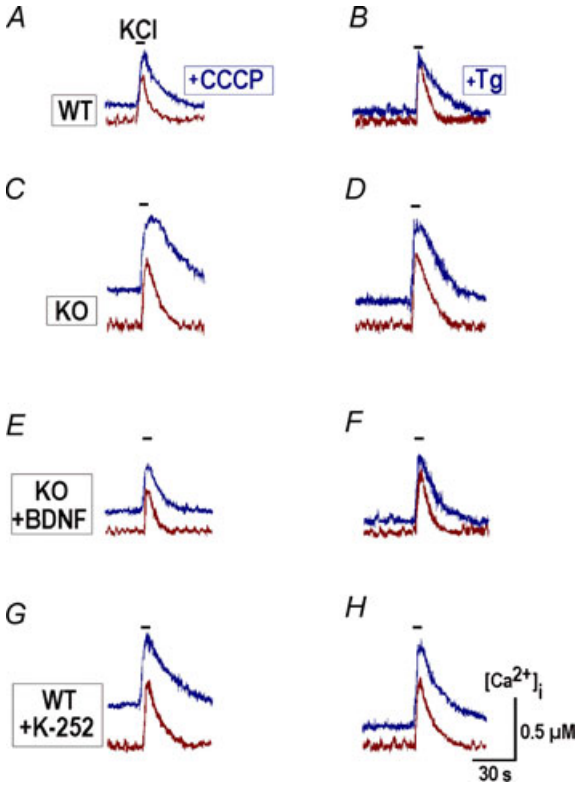

Figure 4. Contributions of mitochondria and ER to the slow calcium buffering in preBötC neurons
Depolarisations with high-K^+ (50 mM) were induced before and 2 min after applications of 1 μM CCCP (*A*, *C*, *E* and *G*) and 1 μM thapsigargin (Tg, *B*, *D*, *F* and *H*). Uncoupling of mitochondria with CCCP and inhibition of SERCA with thapsigargin led to an increase in basal calcium levels and prolonged the decay of calcium transients after membrane depolarisation both in wild-type and KO neurons. After pretreatment with 20 ng ml^{-1} BDNF for 20 min, the time courses of transients in KO neurons were modified and became closer to those measured in WT cells (*E* and *F*). After pretreatment with TrkB blocker 100 nM K252a for 20 min, the transients in WT neurons acquired the amplitudes and decay times typical for KO neurons (*G* and *H*). Mean values of amplitudes and decay times are given in Table 1.

Application of BDNF alone always induced the two effects – an immediate transient increase and subsequent slow $[Ca^{2+}]_i$ decrease (Fig. 5). Both effects were related to Ca^{2+} handling by ER as they did not depend on extracellular Ca^{2+}, were abolished after application of thapsigargin and they were not affected by CCCP. The fast transient to BDNF represents a Ca^{2+} release (Bramham & Messaoudi, 2005; Lang *et al.* 2007), as this effect was not observed after activation of metabotropic receptors with ATP, t-ACPD, or substance P, or in the presence of thapsagargin ($n \geq 4$ for each, data not shown), each of which depletes ER Ca^{2+}. Depolarisation-induced calcium transients recorded during the secondary long-lasting decrease had smaller amplitudes and rates of decay (Fig. 5*B*) and resembled the responses of WT neurons. Application of 100 nM K-252a for 20 min abolished all effects of BDNF on $[Ca^{2+}]_i$ (the last panel in Fig. 5*B*) and K-252b was ineffective ($n = 4$).

Hypoxia and retraction of neurites

In RTT mouse models, respiratory network disturbances can produce brief periods of hypoxia (Viemari *et al.* 2005; Stettner *et al.* 2007). Calcium levels in preBötC neurons in acute slices show a slow increase during oxygen depletion accompanied by depression of the rhythmic respiratory output (Mironov & Langohr, 2005). Because in many cases calcium triggers delayed changes in the morphology of neurons (Wong & Ghosh, 2002; Henley & Poo, 2004; Hua *et al.* 2005; McAllister, 2007), it is important to know whether such global and long-lasting changes in $[Ca^{2+}]_i$ as those produced by hypoxia can modify connections between preBötC neurons.

To examine such effects we firstly produced chemical hypoxia via 200 μM KCN. Its effects on respiratory neurons *in vivo* are identical to oxygen depletion (Brockhaus *et al.* 1993). Similarly to that observed in the functionally intact preparation (Mironov & Langohr, 2005), the neurons in organotypic slices responded with an initial augmentation of activity, followed by a depression developing simultaneously with a calcium increase (Fig. 6). $[Ca^{2+}]_i$ levels slowly returned to control values after hypoxia, this taking much more time for KO than WT neurons. The decay of depolarisation-induced transients after hypoxia was also much slower for KO neurons. Note that after pretreatment of slices with BDNF (lowermost trace in Fig. 6), the two hypoxia-related parameters of calcium homeostasis were practically identical to the WT responses.

After a brief application of chemical hypoxia (KCN) we observed the retraction of neuronal processes (Fig. 7*A*, row 1). The effects developed within 1 h and showed a clear correlation with $[Ca^{2+}]_i$ increases during hypoxia (Fig. 7*B*). The retractions in KO neurons were about twice those of WT neurons. Pretreatment with BDNF produced much smaller effects during subsequent application of hypoxia and they were in a range observed in WT neurons (Fig. 7, row 2). The largest contribution to calcium increases during hypoxia is evoked by efflux of Ca^{2+} from ER and mitochondria (Mironov & Langohr, 2005). The effects of CCCP and thapsigargin on the retraction of neurites were similar to those of hypoxia (rows 3 and 4 in Fig. 7).

Calcium-induced retraction of neurites was observed only for relatively long lasting (~1 min) calcium elevations. Calcium transients elicited by brief depolarisations did not produce noticeable changes. Some neurites were retracted after longer lasting transients occurring in some neurons without any treatment, interrupting the intrinsic activity (Fig. 8*A*). However, such events were extremely seldom, e.g. in the field of view containing approx. 10 neurons, only a few of these events could be recorded within a 1 h observation time (Fig. 8*B*). They were more frequently observed in KO neurons (Fig. 8*B*) where they had larger amplitudes (0.64 ± 0.12 μM) and slower rates of decay (21.2 ± 1.2 s). After such transients the neurites were retracted – the relative decrease in twelve KO neurons was $16 \pm 5\%$ and in six WT neurons was $6 \pm 3\%$ (measured 1 h after the transient). The differences can be explained by bigger amplitudes and durations of spontaneous transients in KO neurons (Fig. 8*A*).

Network modelling

Because shortening of neuronal processes can decrease neuronal connectivity, we examined how the activity of the

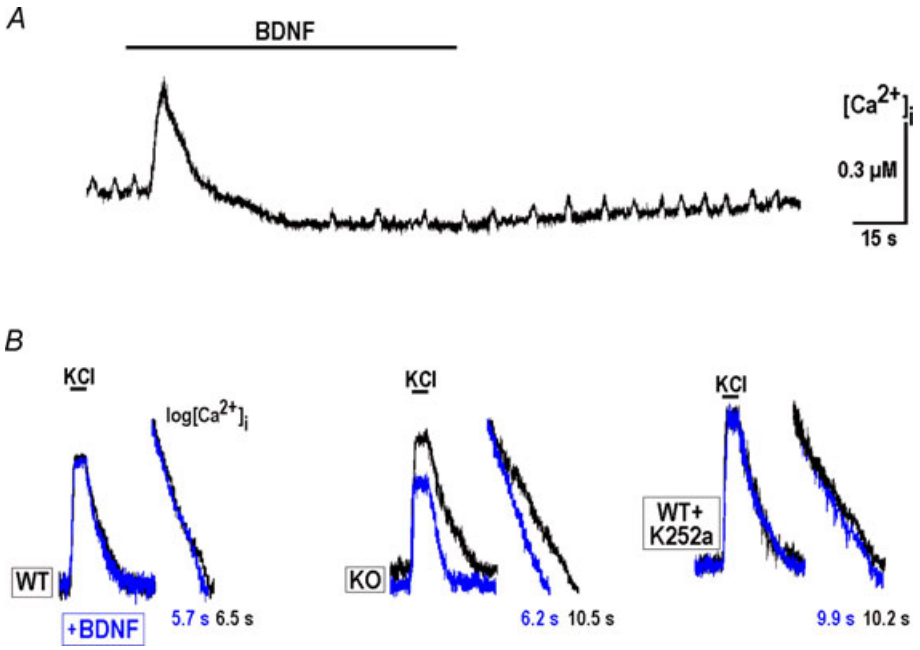

Figure 5. BDNF and calcium homeostasis
A, initial transient increase and long-lasting $[Ca^{2+}]_i$ decrease during BDNF application. *B*, representative calcium transients due to depolarisation recorded at P28 in wild-type and MeCP2 KO slices and in WT slice treated with 100 nM K252a. Semi-log plots near original traces show the differences in $[Ca^{2+}]_i$ recovery times. The traces recorded in the presence of BDNF are shown in grey (online, blue).

network depends on the number of connections between neurons. For this, we used a model proposed to describe respiratory oscillations (Mironov, 2008) and started from a regular network consisting of eight neurons arranged in a ring. Population activity in this configuration showed a stable rhythmic pattern (Fig. 9*A*) with a frequency characteristic of the respiratory network in mice. After rewiring a regular network into a 'small-world' model (Strogatz, 2004) the same activity was observed (Fig. 9*B*). When several connections were removed, the periodic activity persisted but it was occasionally interrupted by bigger and longer lasting transients (Fig. 9*C*). Removal of more connections resulted in a highly irregular activity (Fig. 9*D*).

Note that all neurons and their compartments in these simulations had identical properties and only the neuronal connectivity was varied. Thus, different patterns of activity obtained using this simple generic model came solely from the changes in connectivity. Another important feature is that the model predicts spontaneous 'giant' events that resembles experimentally observed calcium transients (Fig. 8).

Discussion

Rett syndrome is a neurodevelopmental disease caused by improper development of synapses due to the deficit in MeCP2 expression (Francke, 2006; Chahrour & Zoghbi, 2007). After introduction of MeCP2-mutant mice to simulate Rett syndrome (Guy *et al.* 2001), many important issues have been addressed at the cellular and molecular levels that improve our understanding of the pathology of this disease. The major recent findings reveal modification of synapses during the first two weeks of development (Nelson *et al.* 2006; Chao *et al.* 2007), impaired hippocampal plasticity, long-term potentiation (Asaka *et al.* 2006; Moretti *et al.* 2006), breathing irregularities (Viemari *et al.* 2005; Stettner *et al.* 2007), increased neuronal vulnerability during excitotoxicity in the cerebellum (Russell *et al.* 2007) and enhanced susceptibility to hypoxia in the hippocampus (Fischer *et al.* 2008).

The respiratory network is a complex structure containing several nuclei in the lower brainstem (Feldman & Del Negro, 2006). There are at least two

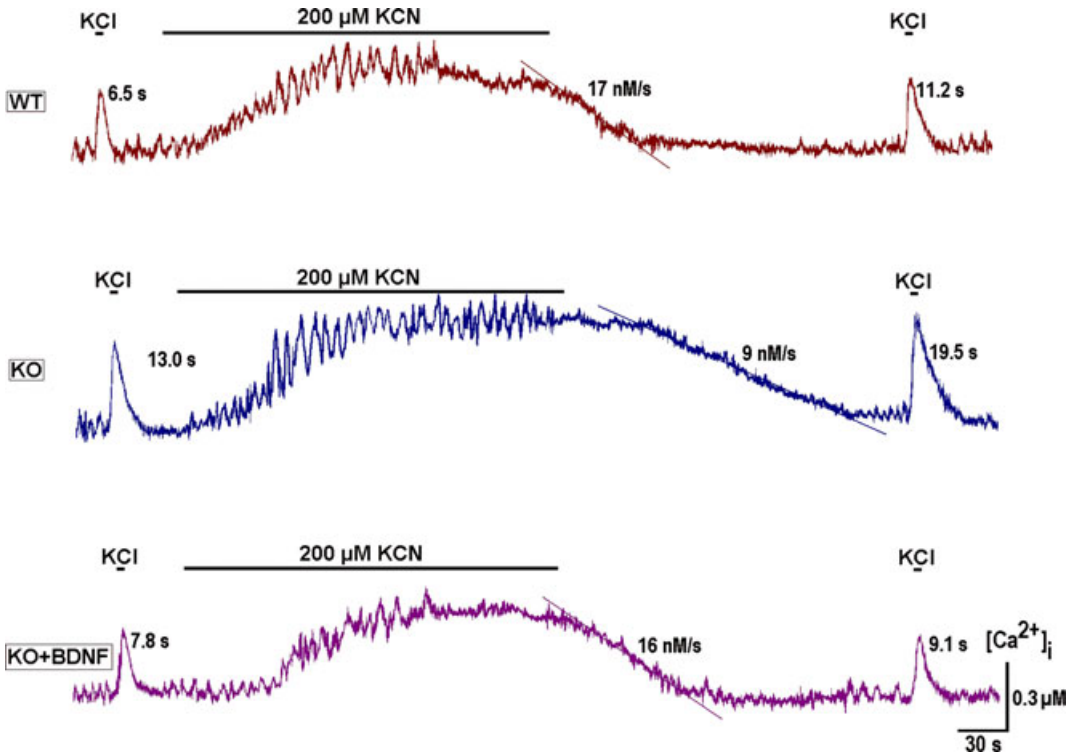

Figure 6. Calcium responses to hypoxia and their modification by BDNF
Chemical hypoxia was induced by KCN (200 μM) and the slow calcium buffering was assessed by applying high-K^+ before and after this treatment. The time constants of $[Ca^{2+}]_i$ decay and the rates of $[Ca^{2+}]_i$ recovery after hypoxia are indicated near each trace. Note the prolonged recovery of calcium levels after hypoxia in neurons from MeCP2 KO mice that was corrected to WT levels after applying 20 ng ml^{-1} BDNF for 20 min. The traces shown are representative of the experiments performed in four different preparations.

identified regions – the pre-Bötzinger complex (Smith *et al.* 1991) and the parafacial respiratory group coupled to the preBötC (Onimaru *et al.* 2006) – which contribute to generation of the respiratory rhythm. Aiming to understand the mechanisms which are involved in abnormal development of the respiratory network in Rett syndrome, we selectively introduced the fluorescent Ca^{2+} sensor protein D3cpv into brainstem slices and found specific alterations in calcium homeostasis in preBötC neurons in the mutant mice. KO neurons had higher resting $[Ca^{2+}]_i$ levels and showed bigger amplitudes and longer decay times of depolarisation-induced calcium transients. Improper regulation of calcium seemingly promotes generation of large-amplitude calcium transients in KO neurons after which neuronal processes are retracted, (Fig. 8) presumably causing a compromised wiring in preBötC in the mutant mice (Fig. 1). Pretreatment with BDNF corrected calcium handling in KO neurons to that typical in WT and pretreatment of KO slices with BDNF largely counteracted with exacerbated retraction of neurites after global calcium transients (Fig. 7). Our data point to SERCA as a target of BDNF-mediated improvement of Ca^{2+} handling in KO neurons consistent with observations of increased Ca^{2+}

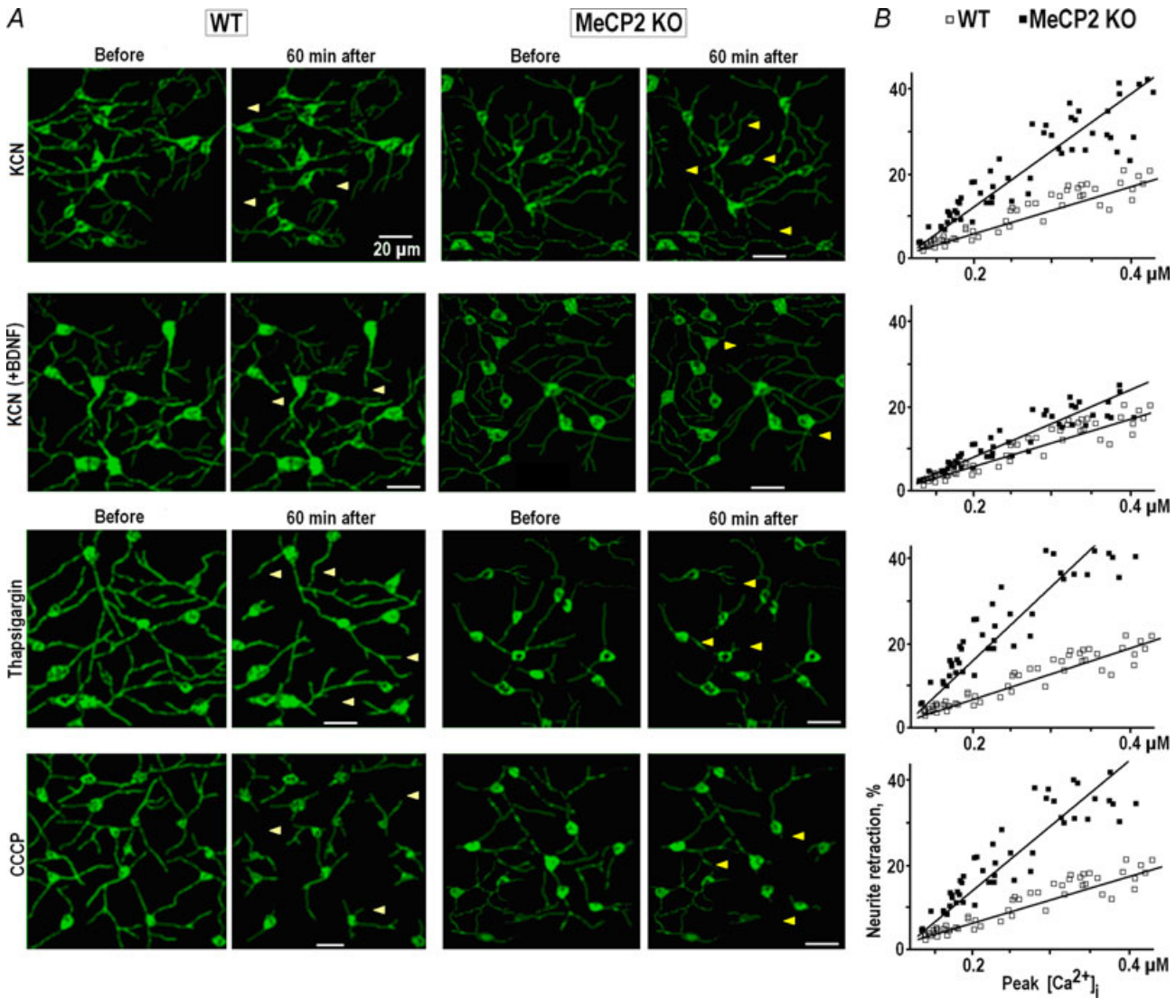

Figure 7. Retraction of neuronal processes after global calcium increases
A, images of the respiratory network in wild-type and MeCP2 KO mice at P28 obtained before and 60 min after application of the agents which produced long-lasting calcium increases – a chemical hypoxia (200 μM KCN) in control and after pretreatment with 20 ng ml^{-1} BDNF for 20 min, 1 μM thapsigargin and 1 μM CCCP. The positions of some retracted processes are indicated by arrowheads. *B*, correlations between relative shortening of the processes and measured peak $[Ca^{2+}]_i$. Straight lines show linear regression of the data (all correlation coefficients are > 0.95).

capacity in ER in cerebellar granule cells pretreated with 10 ng ml^{-1} BDNF (Mhyre *et al.* 2000).

Recent studies document a dynamic regulation of neuronal morphology by calcium (Hua *et al.* 2005; Spitzer *et al.* 2002). Its transient elevations can trigger either elongation or retraction of neuronal processes. The prevalence of one of the two mechanisms is determined by the amplitude, duration and spatial spread of calcium increases. Thus, local fast transients facilitate the attraction of neuronal processes whereas the global long-lasting calcium increases promote their repulsion (Wong & Ghosh, 2002; Ciccolini *et al.* 2003; Henley & Poo, 2004; McAllister, 2007). For example, dendrites in retina are retracted after thapsigargin-induced calcium release from ER (Lohmann *et al.* 2002). Similar effects were observed in preBötC neurons in response to global calcium increases induced by brief hypoxia and Ca^{2+} efflux from ER and mitochondria. The amount of retraction correlated well with the amplitude of the calcium transients (Fig. 7).

The establishment of the dendritic tree is a highly dynamic process characterized by extension and retraction of neuronal processes followed by their stabilization and growth. The early development of dendrites is regulated by cell-intrinsic programmes as well as by molecular signals which control various aspects of dendritic development. Dendrite development and complexity are additionally modulated by intrinsic neuronal activity and calcium plays a key role in these processes (Wong & Ghosh, 2002; Spitzer *et al.* 2002; Henley & Poo, 2004; Hua *et al.* 2005; McAllister, 2007). It is believed that there is an immediate, local response mediated by calcium sensitive signalling via Rho family GTPases that results in alterations of the dendritic cytoskeleton. In addition to the fast local signalling effects of calcium on dendrite

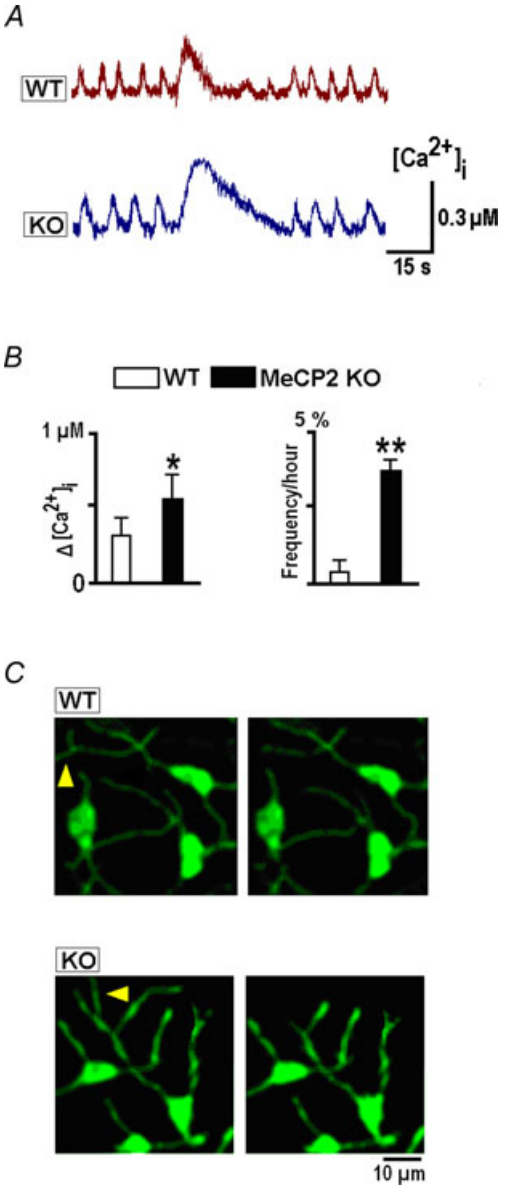

Figure 8. Spontaneous global $[Ca^{2+}]_i$ increases and retraction of neuronal processes
A, selected episodes of spontaneous rhythmic activity interrupted by long-lasting calcium transients. *B*, mean amplitudes and frequencies of observation of these transients. *C*, the images taken before and 60 min after spontaneous transients show the retractions of neuronal processes as indicated by arrowheads.

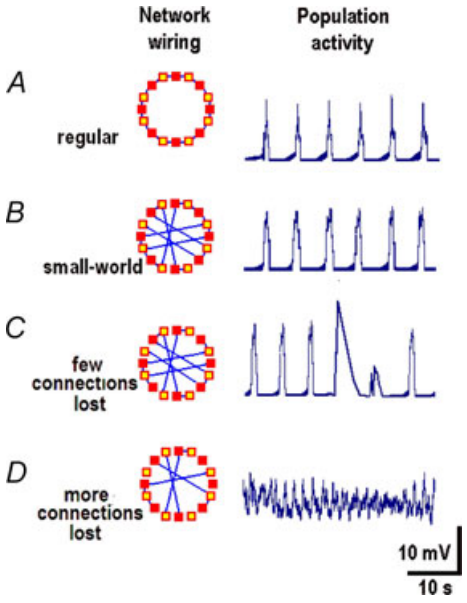

Figure 9. Activity in the model network
Simulations were made using a model of respiratory rhythm generation (Mironov, 2008) which considers the interactions between excitability sites in dendrites (open squares in the insets) and neurons (filled squares). The basic configuration (a regular network) consisted of eight neurones arranged in the ring (*A*) and it was then converted into the small-world model (*B*) by rewiring (Strogatz, 2004). After removal of only a few connections the rhythmic pattern was maintained but it was occasionally interrupted by bigger and longer lasting transients (*C*). Removal of further connections transformed a regular activity into chaotic discharges (*D*).

structure, neuronal activity initiates a delayed, prolonged response on dendrite development. This probably involves activation of calcium/calmodulin-dependent protein kinases (CaMK) and the mitogen activated protein kinase (Ras/MAPK) pathway. Calcium-dependent transcription is also regulated by the calcium-responsive transactivator (CREST), which contributes to the activity-induced expression of genes controlling dendrite morphology. These genes include the candidate plasticity gene-15 (cpg15), Arc, Homer, and BDNF. Decoding how calcium signalling events are coordinated to specify transcription of specific genes and how the proteins encoded by these genes exert specific effects on dendrite morphology are yet to be revealed.

We propose that spontaneous retraction of neuronal processes caused by impaired calcium handling in MeCP2 KO mice can be responsible for the diminished wiring which we observed in preBötC (Fig. 1). Failures in network structure can produce the breathing irregularities characteristic of Rett syndrome. The respiratory network in neonatal mice is estimated to consist of about 600 neurons (Feldman & Del Negro, 2006) and most of these are likely to be redundant, which assures robust generation of the respiratory motor output under most conditions. The simulations in the present study show that a 'small-world' model is as good as a regular model in generating stable rhythmic patterns (Fig. 9). Removal of only a few connections gives rise to big spontaneous transients resembling those observed experimentally (Fig. 8) and further decrease in connectivity within a model produced chaos. Such effects of decreasing neuronal connectivity can be relevant to the appearance and progression of breathing disorders in Rett syndrome. The RTT mouse model is characterised by spontaneous interruptions of breathing activity (Viemari *et al.* 2005; Stettner *et al.* 2007) that increase in severity and incidence. Ensuing brief hypoxia produces global calcium increases and subsequent retraction of some neuronal processes that can decrease neuronal connectivity. Network stability decreases, which in turn promotes new hypoxic episodes and so on, until neuronal connectivity falls below some critical level where no rhythmic pattern can be generated. Consequently, irregular activity appears. In order to prevent this rhythm disruption, appropriate compensatory mechanisms are needed, probably the most important being the BDNF-related signalling pathway, making this factor an important subject for research aiming towards treatment for Rett syndrome (Ogier *et al.* 2007; Larimore *et al.* 2009).

References

Asaka Y, Jugloff DG, Zhang L, Eubanks JH & Fitzsimonds RM (2006). Hippocampal synaptic plasticity is impaired in the Mecp2-null mouse model of Rett syndrome. *Neurobiol Dis* **21**, 217–227.

Berridge MJ, Lipp P & Bootman MD (2000). The versatility and universality of calcium signalling. *Nat Rev Mol Cell Biol* **1**, 11–21.

Bouvier J, Autran S, Dehorter N, Katz DM, Champagnat J, Fortin G & Thoby-Brisson M (2008). Brain-derived neurotrophic factor enhances fetal respiratory rhythm frequency in the mouse preBötzinger complex in vitro. *Eur J Neurosci* **28**, 510–520.

Bramham CR & Messaoudi E (2005). BDNF function in adult synaptic plasticity: the synaptic consolidation hypothesis. *Prog Neurobiol* **76**, 99–125.

Brockhaus J, Ballanyi K, Smith JC & Richter DW. (1993). Microenvironment of respiratory neurons in the in vitro brainstem-spinal cord of neonatal rats. *J Physiol* **462**, 421–445.

Ciccolini F, Collins TJ, Sudhoelter J, Lipp P, Berridge MJ & Bootman MD (2003). Local and global spontaneous calcium events regulate neurite outgrowth and onset of GABAergic phenotype during neural precursor differentiation. *J Neurosci* **23**, 103–111.

Chahrour M & Zoghbi HY (2007). The story of Rett syndrome: from clinic to neurobiology. *Neuron* **56**, 422–437.

Chao HT, Zoghbi HY & Rosenmund C (2007). MeCP2 controls excitatory synaptic strength by regulating glutamatergic synapse number. *Neuron* **56**, 58–65.

Chen WG, Chang Q, Lin Y, Meissner A, West AE, Griffith EC, Jaenisch R & Greenberg ME (2003). Derepression of BDNF transcription involves calcium-dependent phosphorylation of MeCP2. *Science* **302**, 885–889.

Feldman JL & Del Negro CA (2006). Looking for inspiration: new perspectives on respiratory rhythm. *Nat Rev Neurosci* **7**, 232–242.

Fischer M, Reuter J, Gerich FJ, Hildbrandt B, Hägele S, Katschinski D & Mueller M (2008). Enhanced hypoxia susceptibility in hippocampal slices from a mouse model of Rett Syndrome. *J Neurophysiol* **101**, 1016–1032.

Francke U (2006). Mechanisms of disease: neurogenetics of MeCP2 deficiency. *Nat Clin Pract Neurol* **2**, 212–221.

Gaultier C & Gallego J (2008). Neural control of breathing: insights from genetic mouse models. *J Appl Physiol* **104**, 1522–1530.

Grynkiewicz G, Poenie M & Tsien RY (1985). A new generation of Ca^{2+} indicators with greatly improved fluorescence properties. *J Biol Chem* **260**, 3440–3450.

Guy J, Hendrich B, Holmes M, Martin JE & Bird A (2001). A mouse Mecp2-null mutation causes neurological symptoms that mimic Rett syndrome. *Nat Genet* **27**, 322–326.

Hartelt N, Skorova E, Manzke T, Suhr M, Mironova L, Kügler S & Mironov SL (2008). Imaging of respiratory network topology in living brainstem slices. *Mol Cell Neurosci* **37**, 425–431.

Henley J & Poo MM (2004). Guiding neuronal growth cones using Ca^{2+} signals. *Trends Cell Biol* **14**, 320–330.

Hua JY, Smear MC, Baier H & Smith SJ (2005). Regulation of axon growth in vivo by activity-based competition. *Nature* **434**, 1022–1026.

Kügler S, Kilic E & Bahr M (2003). Human synapsin 1 gene promoter confers highly neuron-specific long-term transgene expression from an adenoviral vector in the adult rat brain depending on the transduced area. *Gene Ther* **10**, 337–347.

Lang SB, Stein V, Bonhoeffer T & Lohmann C (2007). Endogenous brain-derived neurotrophic factor triggers fast calcium transients at synapses in developing dendrites. *J Neurosci* **27**, 1097–1105.

Larimore JL, Chapleau CA, Kudo S, Theibert A, Percy AK & Pozzo-Miller L (2009). Bdnf overexpression in hippocampal neurons prevents dendritic atrophy caused by Rett-associated MECP2 mutations. *Neurobiol Dis* (in press).

Lohmann C, Myhr KL & Wong RO (2002). Transmitter-evoked local calcium release stabilizes developing dendrites. *Nature* **418**, 177–181.

Martinowich K, Manji H & Lu B (2007). New insights into BDNF function in depression and anxiety. *Nat Neurosci* **10**, 1089–1093.

McAllister AK (2007). Dynamic aspects of CNS synapse formation. *Annu Rev Neurosci* **30**, 425–450.

Mironov SL (1995). Plasmalemmal and intracellular Ca^{2+} pumps as main determinants of slow Ca^{2+} buffering in rat hippocampal neurones. *Neuropharmacology* **34**, 1123–1132.

Mironov SL (2008). Metabotropic glutamate receptors activate dendritic calcium waves and TRPM channels which drive rhythmic respiratory patterns in mice. *J Physiol* **586**, 2272–2291.

Mironov SL (2009). Respiratory circuits: function, mechanisms, topology and pathology. *Neuroscientist* (in press).

Mironov SL & Langohr K (2005). Mechanisms of Na^{+} and Ca^{2+} influx into respiratory neurons during hypoxia. *Neuropharmacology* **48**, 1056–1065.

Moretti P, Levenson JM, Battaglia F, Atkinson R, Teague R, Antalffy B, Armstrong D, Arancio O, Sweatt JD & Zoghbi HY (2006). Learning and memory and synaptic plasticity are impaired in a mouse model of Rett syndrome. *J Neurosci* **26**, 319–327.

Mhyre TR, Maine DN & Holliday J (2000). Calcium-induced calcium release from intracellular stores is developmentally regulated in primary cultures of cerebellar granule neurons. *J Neurobiol* **42**, 134–147.

Nectoux J, Bahi-Buisson N, Guellec I, Coste J, De Roux N, Rosas H, Tardieu M, Chelly J & Bienvenu T (2008). The p.Val66Met polymorphism in the BDNF gene protects against early seizures in Rett syndrome. *Neurology* **70**, 2145–2151.

Nelson ED, Kavalali ET & Monteggia LM (2006). MeCP2-dependent transcriptional repression regulates excitatory neurotransmission. *Curr Biol* **16**, 710–716.

Ogier M, Wang H, Hong E, Wang Q, Greenberg ME & Katz DM (2007). Brain-derived neurotrophic factor expression and respiratory function improve after ampakine treatment in a mouse model of Rett syndrome. *J Neurosci* **27**, 10912–10917.

Onimaru H, Kumagawa Y, Homma I (2006). Respiration-related rhythmic activity in the rostral medulla of newborn rats. *J Neurophysiol* **96**, 55–61.

Palmer AE, Giacomello M, Kortemme T, Hires SA, Lev-Ram V, Baker D & Tsien RY (2006). Ca^{2+} indicators based on computationally redesigned calmodulin-peptide pairs. *Chem Biol* **13**, 521–530.

Palmer AE & Tsien RY (2006). Measuring calcium signaling using genetically targetable fluorescent indicators. *Nat Protoc* **1**, 1057–1065.

Ruangkittisakul A, Schwarzacher SW, Secchia L, Poon BY, Ma Y, Funk GD & Ballanyi K (2006). High sensitivity to neuromodulator-activated signaling pathways at physiological $[K^{+}]$ of confocally imaged respiratory center neurons in on-line-calibrated newborn rat brainstem slices. *J Neurosci* **26**, 11870–11880.

Russell JC, Blue ME, Johnston MV, Naidu S & Hossain MA (2007). Enhanced cell death in MeCP2 null cerebellar granule neurons exposed to excitotoxicity and hypoxia. *Neuroscience* **150**, 563–574.

Shevtsova Z, Malik JM, Michel U, Bahr M & Kugler S (2005). Promoters and serotypes: targeting of adeno-associated virus vectors for gene transfer in the rat central nervous system in vitro and in vivo. *Exp Physiol* **90**, 53–59.

Smith JC, Ellenberger HH, Ballanyi K, Richter DW & Feldman JL (1991). Pre-Bötzinger complex: a brainstem region that may generate respiratory rhythm in mammals. *Science* **254**, 726–729.

Spitzer NC, Kingston PA, Manning TJ & Conklin MW (2002). Outside and in: development of neuronal excitability. *Curr Opin Neurobiol* **12**, 315–323.

Stettner GM, Huppke P, Brendel C, Richter DW, Gärtner J & Dutschmann M (2007). Breathing dysfunctions associated with impaired control of postinspiratory activity in Mecp2–/y knockout mice. *J Physiol* **579**, 863–876.

Strogatz S (2004). *Sync: The Emerging Science of Spontaneous Order*. Hyperion, London.

Sun YE & Wu H (2006). The ups and downs of BDNF in Rett syndrome. *Neuron* **49**, 321–323.

Turrigiano G (2007). Homeostatic signaling: the positive side of negative feedback. *Curr Opin Neurobiol* **17**, 318–324.

Viemari JC, Roux JC, Tryba AK, Saywell V, Burnet H, Peña F, Zanella S, Bévengut M, Barthelemy-Requin M, Herzing LB, Moncla A, Mancini J, Ramirez JM, Villard L & Hilaire G (2005). Mecp2 deficiency disrupts norepinephrine and respiratory systems in mice. *J Neurosci* **25**, 11521–11530.

Wallace DJ, Meyer zum Alten Borgloh S, Astori S, Yang Y, Bausen M, Kügler S, Palmer AE, Tsien RY, Sprengel R, Kerr JD, Denk W & Hasan MT (2008). Single-spike detection in vitro and in vivo with a genetic Ca sensor. *Nat Methods* **5**, 797–804.

Wang H, Chan SA, Ogier M, Hellard D, Wang Q, Smith C & Katz DM (2006). Dysregulation of brain-derived neurotrophic factor expression and neurosecretory function in Mecp2 null mice. *J Neurosci* **26**, 10911–10915.

Wenk GL (1997). Rett syndrome: neurobiological changes underlying specific symptoms. *Prog Neurobiol* **51**, 383–391.

Wong ROL & Ghosh A (2002). Activity-dependent regulation of dendritic growth and patterning. *Nat Rev Neurosci* **3**, 803–812.

Zhou Z, Hong EJ, Cohen S, Zhao WN, Ho HY, Schmidt L, Chen WG, Lin Y, Savner E, Griffith EC, Hu L, Steen JA, Weitz CJ & Greenberg ME (2006). Brain-specific phosphorylation of MeCP2 regulates activity-dependent Bdnf transcription, dendritic growth, and spine maturation. *Neuron* **52**, 255–269.

Zoghbi HY (2003). Postnatal neurodevelopmental disorders: meeting at the synapse? *Science* **302**, 826–830.

Author contributions

E.S. performed the imaging and carried out the statistical analysis, N.H. designed and produced organotypic slice preparation, M.T.H. and S.K. designed and generated the recombinant AAV-D3cpv virus, L.A.M. analysed the data, designed the mathematical model and performed the simulations, S.K. participated in the design of the study and writing the manuscript, S.L.M. conceived, designed and coordinated the study, performed the imaging, carried out the analysis of the experimental data and wrote the manuscript. All authors have read and approved the final manuscript.

Acknowledgements

The authors thank C. Ludwig for critical reading of the manuscript and helpful comments.